Carbohydrate Polymers 81 (2010) 919–924

Contents lists available at ScienceDirect

Carbohydrate Polymers

journal homepage: www.elsevier.com/locate/carbpol

Preparation of nanofibrillar carbon from chitin nanofibers

M. Nogi [a,*], F. Kurosaki [b], H. Yano [a], M. Takano [b]

[a] Research Institute of Sustainable Humanosphere, Kyoto University, Uji, Kyoto 611-0011, Japan
[b] Institute for Integrated Cell-Material Sciences, Kyoto University, Kyoto 606-8501, Japan

ARTICLE INFO

Article history:
Received 21 August 2009
Received in revised form 27 January 2010
Accepted 7 April 2010
Available online 13 May 2010

Keywords:
Carbon nanofiber
Chitin
Wood cellulose
Surface area
TGA

ABSTRACT

Nanofibrillar carbons were prepared by the carbonization of prawn chitin and wood cellulose nanofibers. Chitin and cellulose nanofibers with the average width of 10 nm were obtained by a grinder treatment from prawn shells and wood cell walls, respectively. Nanofiber aerogels prepared from nanofiber-water suspensions by solvent exchange and freeze-drying were used as carbon precursors. Since chitin nanofibers did not flocculate in organic solvents due to their low hydrophilicity, the aerogels of chitin nanofibers did not form wide bundles of coalesced nanofibers. Furthermore, chitin nanofibers had higher thermal stability than wood cellulose nanofibers. Thus, after the carbonization of chitin nanofibers, the original fine and individual nanofiber network was maintained in the chitin carbon. In contrast, after the carbonization of wood cellulose nanofibers, the original nanofiber morphology was destroyed due to the aggregations of wood cellulose nanofibers and their low thermal stability.

1. Introduction

Chitin and cellulose are the most abundant bioresources on earth—the former is found in arthropods, mollusks, and fungi, and the latter is found in plants. Chitins are a yearly production of approximately 10^{10}–10^{12} tons. However, most of them are discarded as industrial waste without effective utilization (Shahidi & Synowiecki, 1991). Thus, it is important to make efficient use of this biomass resource as a natural and environmentally friendly material.

Recently, chitin and cellulose nanofibers (also known as bionanofibers) with a diameter of 4–20 nm were obtained from squid pens, crustacean exoskeletons, and wood cell walls (Abe, Iwamoto, & Yano, 2007; Fan, Saito, & Isogai, 2008, 2009; Ifuku et al., 2009; Iwamoto, Nakagaito, Yano, & Nogi, 2005; Saito, Nishiyama, Putaux, Vignon, & Isogai, 2006). Moreover, chemical modifications of bionanofibers have also succeeded in the improvement of mechanical properties of bionanofiber materials (Ifuku et al., 2007; Nogi et al., 2006). The bionanofiber materials are the perfect candidate for continuous roll-to-roll processing in the future production of electronic devices, such as flexible displays, solar cells, e-papers, and a myriad of new flexible circuit technologies (Nogi, Iwamoto, Nakagaito, & Yano, 2009; Nogi & Yano, 2008, 2009; Yano et al., 2005).

Thermal transformation of bionanofibers without changing their morphology via calcinations at elevated temperatures is effective procedure to impart new functionalities such as superior mechanical properties, electrical and thermal conductivity, heat and chemical resistance and so on. These properties of carbon fiber make it very popular in aerospace, civil engineering, filter medium, wind generator blades, and sporting goods. However, since most biomasses would be destroyed during carbonization, it is difficult to preserve their nanostructures (Deng, Liao, & Shi, 2008; Paris, Zollfrank, & Zickler, 2005; Polarz, Smarsly, & Schattka, 2002; Yoshino, Matsuoka, & Nogami, 1990). For example, Yoshino et al. (1990) found that when hydrogels of bacterial cellulose nanofibers were oven-dried, the nanofiber morphology was destroyed after graphitization. However, when bacterial and tunicate cellulose nanofiber aerogels with large surface areas, obtained by solvent exchange (water–ethanol–*t*-butyl alcohol) and freeze-drying, were carbonized or graphitized, the nanofiber morphology was maintained without melting (Ishida, Kim, Kuga, Nishiyama, & Brown, 2004; Kim, Nishiyama, Wada, & Kuga, 2001; Kuga, Kim, Nishiyama, & Brown, 2002). Therefore, to carbonize bionanofibers without damaging their nanostructures, it is important to prepare nanofiber aerogels having large surface areas.

To fabricate an aerogel with a large surface area, it is important to disperse bionanofibers homogeneously in organic solvents, in order to prevent fiber flocculation. Chitin is a linear polysaccharide of β-(1-4)-2-acetamido-2-deoxy-D-glucose. The chemical structure of chitin is slightly dissimilar to that of cellulose with a hydroxyl group replaced by an acetamido group. Therefore, chitin appears to have an advantage over cellulose in that chitin nanofibers disperse more homogeneously in organic solvents than cellulose nanofibers do.

* Corresponding author. Present address: Institute of Science and Industrial Research, Osaka University, Ibaraki 567-0047, Japan. Tel.: +81 6 6879 8521; fax: +81 6 6879 8522.
E-mail address: nogi@eco.sanken.osaka-u.ac.jp (M. Nogi).

0144-8617/$ – see front matter © 2010 Elsevier Ltd. All rights reserved.
doi:10.1016/j.carbpol.2010.04.006

In this study, chitin and wood cellulose nanofibers were obtained by grinding water suspensions of purified prawn shells and wood flours, respectively. The nanofiber suspensions were then subjected to solvent exchange and freeze-drying. As a result, chitin nanofibrillar carbon with a large surface area was successfully obtained; however, the original nanofiber morphology was destroyed in wood cellulose nanofibrillar carbon, due to its high hydrophobility and low thermal stability.

2. Experimental and methods

2.1. Chitin and cellulose nanofibers

Chitin nanofibers were obtained from fresh shells of black tiger prawn (*Penaeus monodon*). The prawn shells were first immersed in 50 wt% ethanol solution at 20 °C for 12 h to remove pigments. Then, calcium carbonates in the chitin sample were removed by immersing the sample in 3.6 wt% hydrochloric acid solution at 20 °C for 24 h. Further, proteins in the sample were removed by immersing the sample in 4 wt% sodium hydroxide solution at 20 °C for 12 h. These steps of acid and alkali treatments were repeated four times. For the promotion of nanofibrillation, the pH value of a water slurry containing 1 wt% of the purified chitin sample was adjusted to 3 by using acetic acid (Fan et al., 2008). This slurry was then passed through a grinder once (MKCA6-3; Masuko Sangyo Co., Ltd.) at 1500 rpm (Ifuku et al., 2009).

Wood cellulose nanofibers were obtained from wood flours of Douglas fir (*Pseudotsuga menziesii*) sieved under 60 mesh. Matrix substances of wood flours, such as wax, hemicelluloses, and lignin, were removed by sodium chlorite and potassium hydroxide (Nogi et al., 2009). A water slurry containing 1 wt% of the purified sample was passed through the grinder once (MKCA6-3; Masuko Sangyo Co., Ltd.) at 1500 rpm (Abe et al., 2007; Iwamoto et al., 2005).

2.2. Nanofiber aerogels used as carbon precursors

A water suspension containing chitin or wood cellulose nanofibers was subjected to solvent exchange and freeze-drying. Then, 25 ml of ethanol (purity: 99.0%) and 350 ml of *t*-butyl alcohol (purity: 99.0%) were added to 125 ml of a water suspension of 0.2 wt% nanofiber; the resultant solution was then centrifuged at 35,000 rpm for 5 min. The sediment was redispersed in 500 ml of *t*-butyl alcohol; the resultant solution was centrifuged under the same conditions. The redispersion and centrifugation steps were repeated four times. Finally, 0.05 wt% suspensions contain-

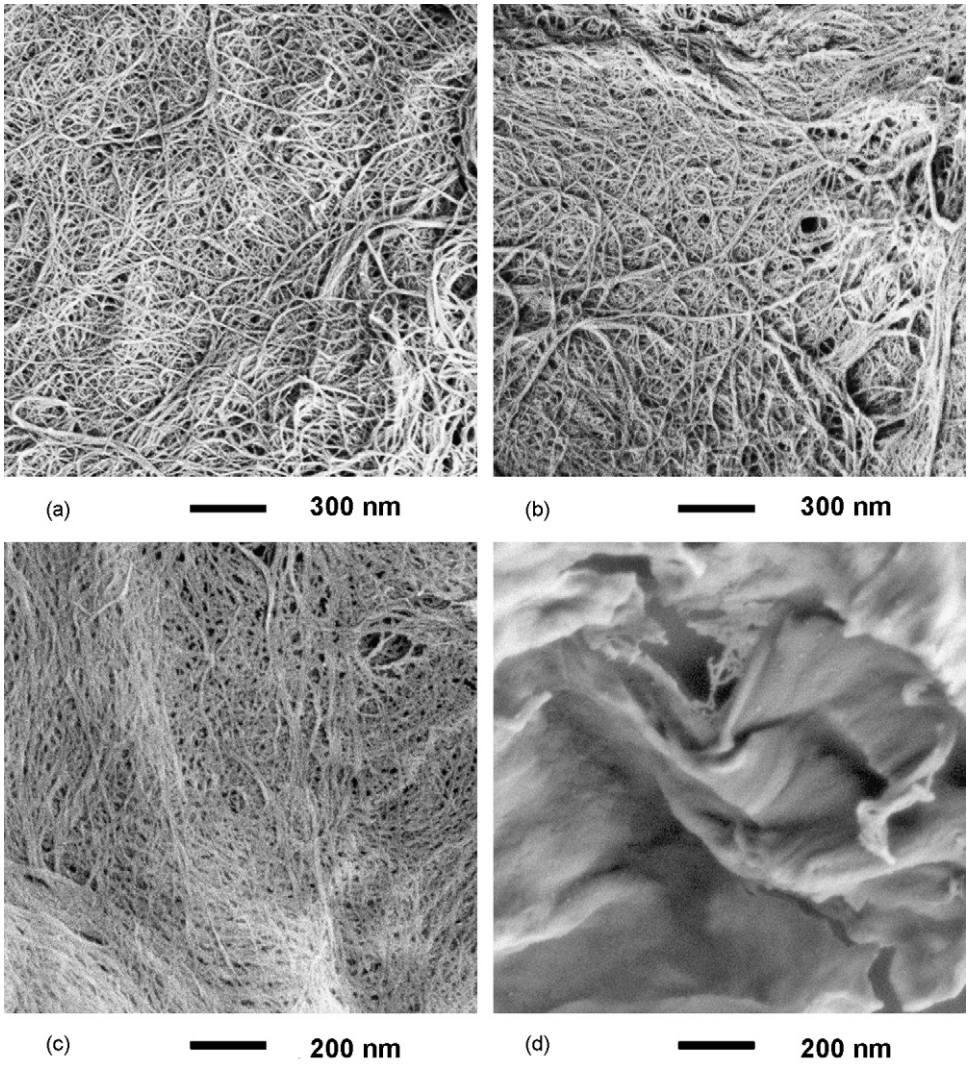

Fig. 1. FE-SEM images of (a) chitin nanofiber aerogel, (b) wood cellulose nanofiber aerogel, (c) chitin carbon, and (d) wood cellulose carbon.

ing *t*-butyl alcohol and a nanofiber (chitin or wood cellulose) were freeze-dried using liquid nitrogen and vacuum-dried overnight at 10–20 Pa.

2.3. Carbonization

The nanofiber samples were carbonized at 600 °C (heating rate: 10 °C/min), and the retention time was 5 min. The flow rate of nitrogen gas was 50 ml/min.

2.4. Analysis and observation of samples

The samples were observed using a field emission scanning electron microscope (FE-SEM) (JSM-6700F; JEOL Ltd.). The samples were coated with Pt (ca. 2 nm) by using an auto fine coater (JFC-1600; JEOL Ltd.). True densities of the chitin and wood cellulose nanofibers were measured using a helium gas pycnometer (Accupyc 1330; Micromeritics Inc.). X-ray diffraction (XRD) patterns of the samples were measured using a diffractometer (RINT2000; Rigaku Corp.) with Ni-filtered Cu-Kα radiation at 40 kV and 40 mA. Elemental compositions of the samples were analyzed using a thermal elemental analyzer (CHN 2400; PerkinElmer Inc.). Nitrogen adsorption/desorption isotherms at 77 K were obtained using a surface area analyzer (Trister 3000; Shimazu Corp.). The samples were outgassed at 105 °C for 2 h under vacuum. The Brunauer–Emmett–Teller (BET) surface areas of the samples were calculated using the BET equation (Brunauer, Emmett, & Teller, 1938); their external surface areas were evaluated using the *t*-plot method (Gregg & Sing, 1982). Thermogravimetric (TG) analysis of the samples was carried out using a TGA2050 analyzer (TA Instruments) in nitrogen atmosphere. The scan rate was 10 °C/min. The α-cellulose content, which was the index of the cellulose purity, was determined by extraction with 17.5 wt% NaOH.

3. Results and discussions

3.1. Freeze-dried aerogels of chitin and wood cellulose nanofibers

Chitin and wood cellulose nanofibers of approximately 10 nm width, which were the bundles of their microfibrils of 2–5 nm width, were obtained by grinding purified shells of black tiger prawn and purified wood flours of Douglas fir (Fig. 1a and b). XRD profiles of chitin and wood cellulose nanofibers are shown in Fig. 2. The XRD profile of chitin nanofibers showed four diffraction peaks at 9.5°, 19.5°, 20.9°, and 23.4°, which corresponded to (0 2 0), (1 1 0), (1 2 0), and (1 3 0) planes, respectively; these are typical crystal patterns of α-chitin (Minke & Blackwell, 1978). Further, the XRD profile of wood cellulose nanofibers showed four diffraction peaks at 14.6°, 16.5°, 22.5°, and 34.6°, which corresponded to (1 −1 0), (1 1 0), (2 0 0), and (0 0 4) planes, respectively; these are typical crystal patterns of cellulose I (Woodcock & Sarko, 1980).

Nanofiber aerogels to be used as carbon precursors were prepared from nanofiber-water suspensions by subjecting the suspensions to (1) precise solvent exchange from water to *t*-butyl alcohol and (2) freeze-drying. As a result, both the aerogels showed fine nanofiber networks. However, wood cellulose nanofibers slightly form wide bundles of coalesced nanofibers (Fig. 1b), while chitin nanofibers showed individual nanofibers without aggregations (Fig. 1a).

To evaluate the dispersion of chitin and wood cellulose nanofibers in aerogels, the theoretical specific surface areas of these

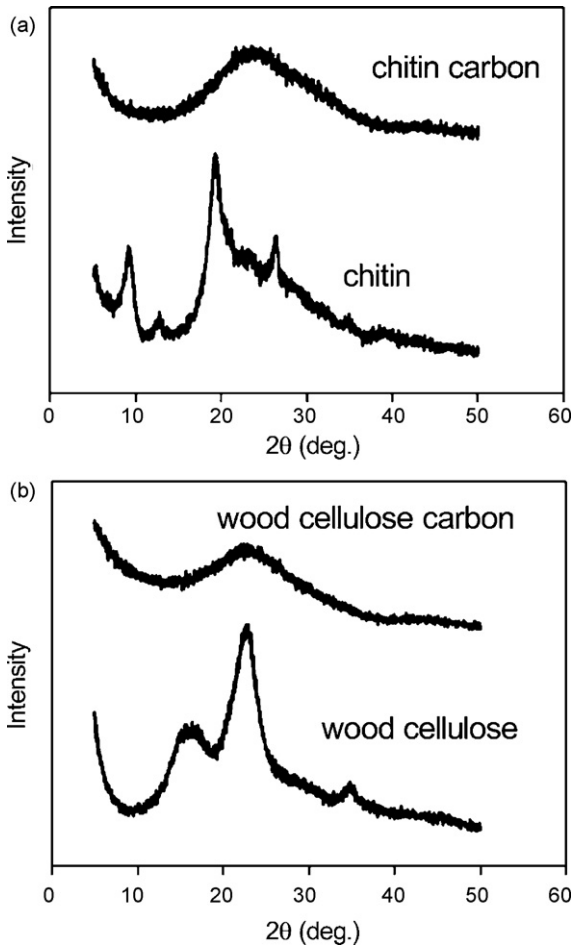

Fig. 2. X-ray diffraction profiles of (a) chitin nanofibers and chitin carbon and (b) wood cellulose nanofibers and wood cellulose carbon.

nanofibers were determined by the followed equation.

$$\text{Theoretical surface area } (m^2/g) = \frac{\text{surface are } (m^2)}{\text{weight } (g)} = \frac{\text{surface are}}{(\text{volume} \times \text{true density})} = \frac{2\pi rL + 2\pi r^2}{\pi r^2 L\rho} = \frac{2}{r\rho}$$

(since the fiber length (L) is significant larger than the radius (r), $2/L\rho$ equals to zero)

where r is radius of bionanofibers (chitin: 10 nm and cellulose: 10 nm), L is length of bionanofibers, and ρ is true density of bionanofibers (chitin: 1.44 g/cm^3 and cellulose: 1.55 g/cm^3). The theoretical surface areas of chitin and wood cellulose nanofibers were determined to be 278 m^2/g and 258 m^2/g, respectively (Fig. 3; open bars). The BET surface areas of the chitin and wood cellulose aerogels were calculated from their nitrogen adsorption/desorption isotherms, and these values were 260 m^2/g and 196 m^2/g, respectively (Fig. 3; gray bars). In other words, the BET surface areas of the chitin and wood cellulose aerogels were 93% and 76% of their corresponding theoretical surface areas, respectively. It is noteworthy that the wood cellulose nanofibers in the

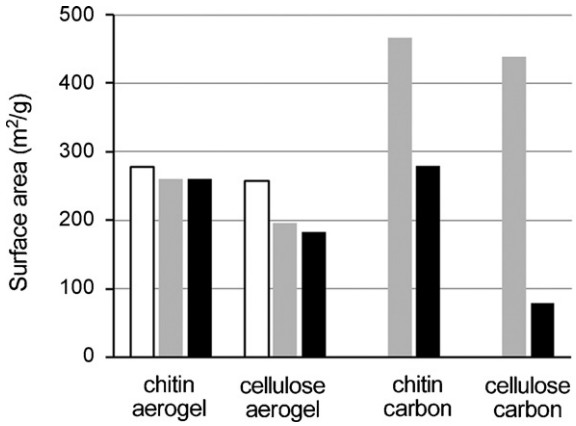

Fig. 3. Surface areas of chitin nanofiber aerogel, wood cellulose nanofiber aerogel, chitin carbon, and wood cellulose carbon (open bars: theoretical surface area; gray bars: BET surface area; solid bars: external surface area).

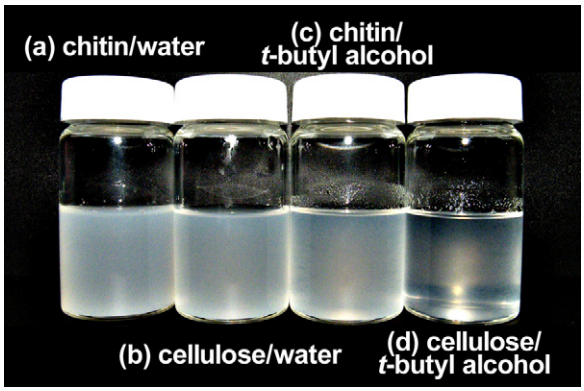

Fig. 4. Photographs of dispersions of chitin and wood cellulose nanofibers in water and the organic solvent. (a) Water suspensions of 0.2 wt% chitin nanofibers, (b) water suspensions of 0.2 wt% wood cellulose nanofibers, (c) *t*-butyl alcohol suspensions of 0.2 wt% chitin nanofibers, and (d) *t*-butyl alcohol suspensions of 0.2 wt% wood cellulose nanofibers.

aerogels coalesced with each other, although the fiber aggregation could not be observed apparently using the FE-SEM.

3.2. Carbonization of chitin and wood cellulose nanofiber aerogels

As shown in Table 1, the carbon contents of the used chitin and wood cellulose nanofibers before heat treatment were 44.7% and 41.7%, respectively. After heat treatment, the carbon content of the wood cellulose nanofibers increased to 86.2%. Further, after heat treatment, the carbon content of the chitin nanofibers increased to 83.1% and the nitrogen content increased slightly from 6.2% to 8.1%, because nitrogen atoms of the acetamide groups remained even after heat treatment. XRD profiles of the chitin and wood cellulose carbon showed broad peaks at $2\theta = 23–25^\circ$ (Fig. 2). From these results, it was confirmed that on being subjected to heat treatment, chitin and cellulose nanofibers were carbonized to form amorphous carbons.

After carbonization, the volume of chitin nanofiber aerogels reduced to less than half of the original volume. Despite this considerable reduction, the original fine network morphology of the carbonized chitin nanofibers was observed to be maintained, as shown in Fig. 1a and c. The appearances of nanofiber network before and after carbonization appear similar. However, the scale bar in Fig. 1a is 300 nm, whereas that in Fig. 1c is 200 nm. Thus, the diameter of chitin nanofibers decreased after carbonization. In contrast, after carbonization, the volume of wood cellulose nanofiber aerogels reduced to less than one-third of the original volume. In addition to this drastic reduction, after carbonization, the original network morphology of wood cellulose nanofibers was entirely destroyed (Fig. 1d).

Kuga et al. reported that after the carbonization of bacterial cellulose nanofiber aerogels with large surface areas, achieved by solvent exchange and freeze-drying, their nanofiber morphology was maintained and the crystal size of bacterial cellulose graphite was half of that of original BC (Kim et al., 2001; Kuga et al., 2002). In case of chitin, we confirmed that their diameter decreased to less than 10 nm after their carbonization as shown in Fig. 1. At present, carbon nanofibers produced by vapor growing or carbonization of electrospun nanofibers have a diameter of 50–300 nm (Al-Saleh & Sundararaj, 2009; Liu, Yue, & Fong, 2009). Since the bionanofibers such as bacterial cellulose and chitin nanofibers can produce the carbon nanofiber comparable to a diameter of multi-walled carbon nanotubes, the bionanofibers are the momentous materials for the production of thinner carbon nanofibers.

Table 1
Elemental analysis of chitin and wood cellulose.

	Carbon (%)	Hydrogen (%)	Nitrogen (%)	Oxygen (%)
Chitin	44.7	7.3	6.2	41.8
Cellulose	41.7	7.7	0.0	50.6
Chitin carbon	83.1	1.1	8.1	7.7
Cellulose carbon	86.2	2.4	0.0	11.4

3.3. Nanofiber morphology after carbonization

The original nanofibrillar morphology was maintained in chitin carbon and destroyed in wood cellulose carbon. Here, we discuss the reasons for this behavior.

To carbonize bionanofibers without destroying their nanostructures, it is important to prepare aerogels with large surface areas. Thus, bionanofibers should be homogeneously dispersed in organic solvents without any aggregations. Fig. 4 shows the just stirred suspensions of 0.2 wt% nanofibers. Fig. 4a and b presents the water suspensions of chitin and wood cellulose nanofibers, respectively. Fig. 4c and d presents the *t*-butyl alcohol suspensions of chitin and wood cellulose nanofibers, respectively. Among them, *t*-butyl alcohol suspensions of wood cellulose nanofibers are obviously different. The suspension exhibits high transparency because the wood cellulose nanofibers aggregate the visible-sized particles in *t*-butyl alcohol.

Chitin and wood cellulose nanofibers obtained from prawn shells and wood flours, respectively, were homogeneously dispersed in water suspensions and their appearances are uniform translucent (Fig. 4a and b). Chitin nanofibers with low hydrophilicity are also dispersed individually in organic solvents during solvent exchange (Fig. 4c). As a result, the original nanofiber morphology of carbonized chitin nanofiber aerogels with large surface areas comparable to the theoretical surface areas was maintained (Figs. 1c and 3). In contrast, when hydrophilic cellulose nanofibers are dipped in organic solvents, they flocculate due to their lower affinities with alcohols (Fig. 4d). Therefore, in our study, wood cellulose carbon did not show nanofiber morphology (Fig. 1d).

There is one more reason why the nanofiber morphology of wood cellulose nanofibers was not retained after their carbonization, explained as follows. TG analysis of chitin and wood cellulose nanofibers was carried out in nitrogen atmosphere up to 600 °C (Fig. 5). Wood cellulose nanofibers began to degrade from around 200 °C, and their derivative thermogravimetric (DTG) peak was observed at 334 °C. Wood cellulose nanofibers obtained from wood flours had an α-cellulose content of only 78.1% because hemicelluloses (matrix substance) were retained after purifying treatment. Thermal decomposition of cellulose and hemicelluloses

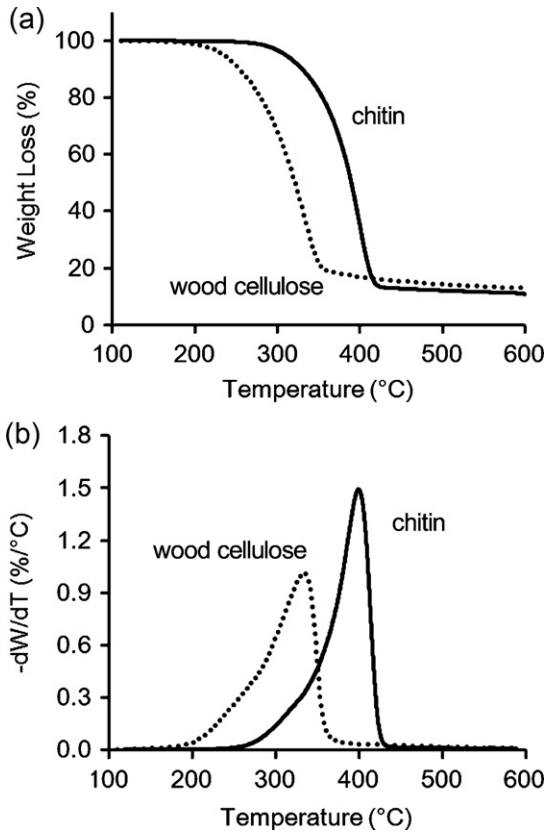

Fig. 5. (a) TG and (b) DTG curves of chitin and wood cellulose nanofibers.

occurs at around 350–365 °C and 200–300 °C (Albano, Gonzalez, Ichazo, & Kaiser, 1999; Byrne & Nagle, 1997). In contrast, chitin nanofibers showed higher thermal stability and began to degrade from around 280 °C, and their DTG peak was observed at 400 °C. These TGA results suggested that before the carbonization of cellulose, substances with low thermal stability, such as hemicelluloses, decomposed and filled the gaps of the nanofiber networks. Therefore, when the hydrophobicity and thermal stability of wood cellulose will be improved by chemical modification, nanofibrillar carbon can be obtained from wood cellulose. We have already confirmed it, and the findings will be reported and discusses elsewhere.

3.4. Surface areas

Carbonization of bionanofibers is expected to result in the formation of carbons with large surface areas, which have potential applications in filter media, tissue engineering scaffolds, electric double-layer capacitors, highly efficient catalysts, and so on. As the external surface area increased, the activity and lifetime of catalysis or filters improved (Suzuki, Namba, & Yashima, 1983; Yamamura, Chaki, Wakatsuki, Okado, & Fujimoto, 1994). As for the carbons with high external surface area, BET surface area can be increased further by physical or chemical activation since the micro pores are developed by the treatments. Thus, high external surface area is one of the anticipated characteristics for nanofibrillar carbons.

The surface areas of chitin and cellulose carbons are shown in Fig. 3. After carbonization, chitin carbon was found to have an external surface area of 279 m^2/g. It was almost constant compared to that of chitin aerogels, because the original nanofibrillar morphologies were maintained in chitin carbon. In contrast, the external surface area of wood cellulose carbon decreased drastically from 183 m^2/g to 78 m^2/g, because the original nanofiber morphology was not retained in it.

4. Conclusion

Chitin and wood cellulose nanofibers, each with a diameter of 10 nm, were obtained by grinding shrimp shells and wood flours, respectively. Chitin nanofibers did not aggregate with each other in carbon precursor aerogels and exhibited high thermal stability; therefore, chitin carbon was shown to have a fine network comprising nanofibers with reduced diameter. On the other hand, wood cellulose nanofibers melted after carbonization, due to their low thermal stability and coagulation in the aerogels. As a result, the external surface area of chitin carbon was three times that of wood cellulose carbon. When the nanofibrillar chitin carbon is activated by physical or chemical treatment such as that with H_2O or NaOH, chitin carbon with a large surface area is obtained, which can have potential applications in filter media, electric double-layer capacitors, highly efficient catalysts, and so on. Finally, when the hydrophobicity or thermal stability of cellulose can be improved by chemical modification, nanofibrillar carbon can be obtained from wood cellulose, which is one of the most abundant biomasses in nature.

Acknowledgment

The first and second authors were supported by a Grant-in-Aid for Scientific Research from Research Fellowships of the Japan Society for the Promotion of Science for Young Scientists.

References

Abe, K., Iwamoto, S., & Yano, H. (2007). Obtaining cellulose nanofibers with a uniform width of 15 nm from wood. *Biomacromolecules*, *8*, 3276–3278.
Albano, C., Gonzalez, J., Ichazo, M., & Kaiser, D. (1999). Thermal stability of blends of polyolefins and sisal fiber. *Polymer Degradation and Stability*, *66*, 179–190.
Al-Saleh, M. H., & Sundararaj, U. (2009). A review of vapor grown carbon nanofiber/polymer conductive composites. *Carbon*, *47*, 2–22.
Brunauer, S., Emmett, P. H., & Teller, E. (1938). Adsorption of gases in multimolecular layers. *Journal of the American Chemical Society*, *60*, 309–319.
Byrne, C. E., & Nagle, D. C. (1997). Carbonization of wood for advanced materials applications. *Carbon*, *35*, 259–266.
Deng, D., Liao, X., & Shi, B. (2008). Synthesis of porous carbon fibers from collagen fiber. *ChemSusChem*, *1*, 298–301.
Fan, Y., Saito, T., & Isogai, A. (2008). Preparation of chitin nanofibers from squid pen β-chitin by simple mechanical treatment under acid conditions. *Biomacromolecules*, *9*, 1919–1923.
Fan, Y., Saito, T., & Isogai, A. (2009). TEMPO-mediated oxidation of β-chitin to prepare individual nanofibrils. *Carbohydrate Polymers*, *77*, 832–838.
Gregg, S. J., & Sing, J. S. W. (1982). *Adsorption, surface area and porosity* (2nd ed.). New York: Academic Press.
Ifuku, S., Nogi, M., Abe, K., Handa, K., Nakatsubo, F., & Yano, H. (2007). Surface modification of bacterial cellulose nanofibers for property enhancement of optically transparent composites: Dependence of acetyl-group DS. *Biomacromolecules*, *8*, 1973–1978.
Ifuku, S., Nogi, M., Abe, K., Yoshioka, M., Morimoto, M., Saimoto, H., & Yano, H. (2009). Preparation of chitin nanofibers with a uniform width as α-chitin from crab shells. *Biomacromolecules*, *10*, 1584–1588.
Ishida, O., Kim, D. Y., Kuga, S., Nishiyama, Y., & Brown, R. M., Jr. (2004). Microfibrillar carbon from native cellulose. *Cellulose*, *11*, 475–480.
Iwamoto, S., Nakagaito, A. N., Yano, H., & Nogi, M. (2005). Optically transparent composites reinforced with plant fiber-based nanofibers. *Applied Physics A*, *81*, 1109–1112.
Kim, D. Y., Nishiyama, Y., Wada, M., & Kuga, S. (2001). Graphitization of highly crystalline cellulose. *Carbon*, *39*, 1051–1056.
Kuga, S., Kim, D. Y., Nishiyama, Y., & Brown, R. M., Jr. (2002). Nanofibrillar carbon from native cellulose. *Molecular Crystals and Liquid Crystals*, *387*, 237–243.
Liu, J., Yue, Z., & Fong, H. (2009). Continuous nanoscale carbon fibers with superior mechanical strength. *Small*, *5*, 536–542.
Minke, R., & Blackwell, J. (1978). The structure of α-chitin. *Journal of Molecular Biology*, *120*, 167–181.
Nogi, M., Abe, K., Handa, K., Nakatsubo, F., Ifuku, S., & Yano, H. (2006). Property enhancement of optically transparent bionanofiber composites by acetylation. *Applied Physics Letters*, *89*, 233123.
Nogi, M., Iwamoto, S., Nakagaito, A. N., & Yano, H. (2009). Optically transparent nanofiber paper. *Advanced Materials*, *21*, 1595–1598.

Nogi, M., & Yano, H. (2008). Transparent nanocomposites based on cellulose produced by bacteria offer potential innovation in the electronics device industry. *Advanced Materials*, *20*, 1849–1852.

Nogi, M., & Yano, H. (2009). Optically transparent nanofiber sheets by deposition of transparent materials—A concept for a roll-to-roll processing. *Applied Physics Letters*, *94*, 233117.

Paris, O., Zollfrank, C., & Zickler, G. A. (2005). Decomposition and carbonisation of wood biopolymers—A microstructural study of softwood pyrolysis. *Carbon*, *43*, 53–66.

Polarz, S., Smarsly, B., & Schattka, J. H. (2002). Hierarchical porous carbon structures from cellulose acetate fibers. *Chemistry of Materials*, *14*, 2940–2945.

Saito, T., Nishiyama, Y., Putaux, J. L., Vignon, M., & Isogai, A. (2006). Homogeneous suspensions of individualized microfibrils from TEMPO-catalyzed oxidation of native cellulose. *Biomacromolecules*, *7*, 1687–1691.

Shahidi, F., & Synowiecki, J. (1991). Isolation and characterization of nutrients and value-added products from snow crab (*Chinoecetes opilio*) and shrimp (*Pandalus borealis*) processing discards. *Journal of Agricultural and Food Chemistry*, *39*, 1527–1532.

Suzuki, I., Namba, S., & Yashima, T. (1983). Determination of external surface area of ZSM-5 type zeolite. *Journal of Catalysis*, *81*, 485–488.

Yamamura, M., Chaki, K., Wakatsuki, T., Okado, H., & Fujimoto, K. (1994). Synthesis of ZSM-5 zeolite with small crystal size and its catalytic performance for ethylene oligomerization. *Zeolite*, *14*, 639–649.

Yano, H., Sugiyama, J., Nakagaito, A. N., Nogi, M., Matsuura, T., Hikita, M., & Handa, K. (2005). Optically transparent composites reinforced with networks of bacterial nanofibers. *Advanced Materials*, *17*, 153–155.

Yoshino, K., Matsuoka, R., & Nogami, K. (1990). Graphite film prepared by pyrolysis of bacterial cellulose. *Journal of Applied Physics*, *68*, 1720–1725.

Woodcock, C., & Sarko, A. (1980). Packing analysis of carbohydrates and polysaccharides. 11. Molecular and crystal structure of native ramie cellulose. *Macromolecules*, *13*, 1183–1187.